Lecture 32 Plasmonics (Introduction)

Review of metal properties

Let us review the properties of metals as they were first described in Lecture 3. The AC conductivity of "Drude metal"

$$\sigma(\omega) = \frac{Ne^2}{m_0(\gamma - j\omega)} = \frac{\sigma_{DC}}{1 - j\omega/\gamma} \tag{32.1}$$

where DC conductivity is

$$\sigma_{DC} = Ne^2 / m_0\gamma \tag{32.2}$$

and damping constant is $\gamma = 1/\tau$ where τ is scattering time. The dielectric constant is then

$$\varepsilon_r = \varepsilon_{rb} + j\sigma(\omega)/\varepsilon_0\omega = \varepsilon_{rb} + j\frac{Ne^2}{\varepsilon_0 m_0\omega(\gamma - j\omega)} = \varepsilon_{rb} - \frac{\omega_p^2}{\omega^2 + j\omega\gamma} \tag{32.3}$$

where plasma frequency is

$$\omega_p = \sqrt{\frac{Ne^2}{\varepsilon_0 m_0}} \tag{32.4}$$

The dispersion of real and imaginary parts fo dielectric constant is shown in Fig.32.1, and is characterized by the fact that for $\omega < \omega_p/\sqrt{\varepsilon_{rb}}$ ($\lambda > \lambda_p\sqrt{\varepsilon_{rb}}$) real part of dielectric constant $\varepsilon_r < 0$ which means the electromagnetic waves cannot propagate inside the metal and get reflected.

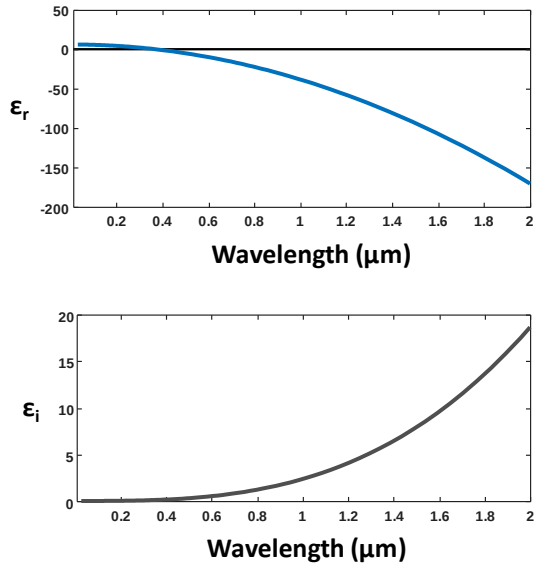

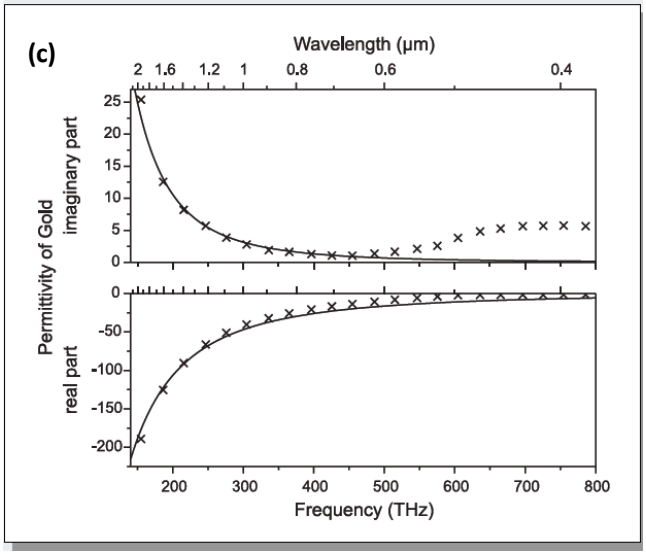

Figure 32.1 Dispersion of (a) real and (b) imaginary parts of the ideal Drude metal dielectric constant (c) Same for the realistic metal –gold

The values of plasma frequencies and damping constants are given in the table 32.1.

	Plasma frequency		Scattering rate
Au	**2081 THz**	**8.5 eV**	**12.3×10^{13} s^{-1}**
Ag	**2182 THz**	**9.0 eV**	**3.2×10^{13} s^{-1}**
Al	**3231 THz**	**13.2 eV**	**27.3×10^{13} s^{-1}**

Table 32.1 Plasma frequencies and damping rates of real metals

Note that plasma frequencies are typically in the deep UV region and scattering rates are on the scale of 1/10fs. In Fig.32.1© the dispersion of real and imaginary parts of dielectric constant of gold is shown. The solid lines correspond to the Drude approximation, and crosses to the experimental data. As one can see the imaginary part of dielectric constant increases beyond 500THz (600nm) due to the interband absorption which renders gold not so useful at shorter wavelengths

Bulk plasmons

. Let us re-write the equation (32.3) as

$$\varepsilon_r = \varepsilon_{rb}\left(1-\frac{\omega_{ps}^2}{\omega^2+j\omega\gamma}\right) \tag{32.5}$$

where we introduced the "screened plasma frequency" as

$$\omega_{ps} = \omega_p / \sqrt{\varepsilon_{rb}} \tag{32.6}$$

If we neglect damping, $\varepsilon_r(\omega_{ps}) = 0$

Let us recall Maxwell's equation (for isotropic medium)

$$\nabla\cdot\mathbf{D} = \mathbf{k}\cdot\mathbf{D} = \varepsilon_0\varepsilon_r(\omega)\mathbf{k}\cdot\mathbf{E} = 0 \tag{32.7}$$

According to this, the solution is transverse wave, $\mathbf{k}\cdot\mathbf{E} = 0$. But there exists another, longitudinal solution where displacement is simply zero,

$$\mathbf{k}\,||\,\mathbf{E}\ \ \mathbf{D}=0\ \ \varepsilon_r(\omega_{ps}) = 0 \tag{32.8}$$

i.e. at only one frequency ω_{ps}. We can write the field of longitudinal wave as

$$\mathbf{E}_{pl} = E_z\hat{\mathbf{z}}e^{j(k_z z-\omega t)} \tag{32.9}$$

Recalling another Maxwell equation,

$$\nabla \times \mathbf{E} = -\mu \frac{\partial \mathbf{H}}{\partial t} \tag{32.10}$$

we see that curl of the longitudinal field is zero (the field is "irrotational") and magnetic field is equal to zero. Let us now find the wavevector of longitudinal wave. For that we consider the metal as a dielectric with dielectric constant ε_{rb} and the charges whose density distribution is $\rho(\mathbf{r})$. Then we can write Gauss's law as

$$\nabla \cdot \varepsilon_0 \varepsilon_{rb} \mathbf{E} = \varepsilon_0 \varepsilon_{rb} \nabla \cdot \mathbf{E} = \rho \tag{32.11}$$

and substituting (32.9) obtain

$$\rho = \varepsilon_0 \varepsilon_{rb} \nabla \cdot \mathbf{E}_{pl} = j \varepsilon_0 \varepsilon_{rb} E_z k_z e^{j(k_z z - \omega t)} \tag{32.12}$$

i.e. we have charge oscillations that are shifted in phase by 90 degrees relative to the electric field as shown in Fig.32.2 (a). The density of electrons is then

$$N(z,t) = N - j \frac{\varepsilon_0 \varepsilon_{rb}}{e} E_z k_z e^{j(k_z z - \omega t)} \tag{32.13}$$

It has the constant value and then oscillating component. The electric current caused by the plasmon field is

$$J_z = \sigma(\omega) E_{pl} = j \frac{Ne^2}{m_0 \omega} E_{pl} = j \frac{Ne^2}{m_0 \omega} E_z e^{j(k_z z - \omega t)} \tag{32.14}$$

Now, invoke the continuity equation

$$\frac{d\rho}{dt} = -\nabla \cdot \mathbf{J} = -\frac{dJ_z}{dz} \tag{32.15}$$

Substituting the charge density from (32.12) and current density from (32.14) we obtain

$$\omega \varepsilon_0 \varepsilon_{rb} E_z k_z e^{j(k_z z - \omega t)} = k_z \frac{Ne^2}{m_0 \omega} E_z e^{j(k_z z - \omega t)} \tag{32.16}$$

which after cancellation of field and wavevector yields

$$\omega = \sqrt{\frac{Ne^2}{\varepsilon_0 \varepsilon_{rb} m_0}} = \omega_{ps} \tag{32.17}$$

indicating that any wavevector is possible and the dispersion curve $\omega(k) = \omega_{ps}$ is flat as shown in Fig.32.2b and actually goes to very high wavevectors, well beyond the diffraction limit. Also note that the group velocity is zero, $v_g = d\omega / dk = 0$ as well as the energy flow is also zero s $\mathbf{S} = \mathbf{E} \times \mathbf{H} = 0$, since the magnetic field is zero. This is a quasi-static wave which can be thought of as two coupled waves- electric field wave and charge density wave.

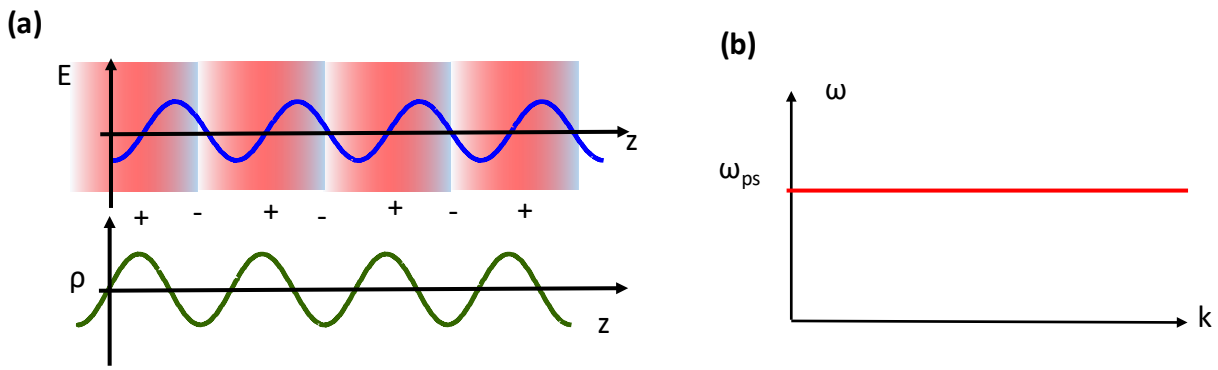

Figure 32.2 (a) Charge density wave in bulk plasmon (b) Dispersion of bulk plasmon

Origin of bulk plasmons

Consider a large volume of metal with surface area S l. What happens if we move all the electrons by a small distance Δz , as shown in Fig.32.3? Then on the right hand side we shall accumulate negative charge

$$Q_s = -eS\Delta zN \tag{32.18}$$

and on the left hand side equal charge of opposite sign due to the positively charged ions exposed by the electrons that have moved to the right.

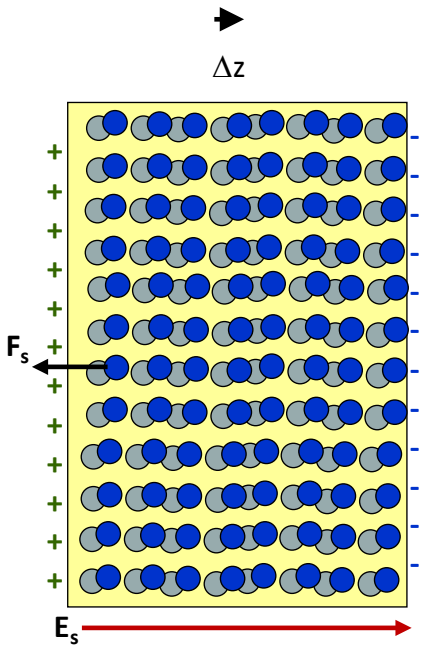

Figure 32.3 The origin of longitudinal charge oscillations.

The surface charge than gives rise to the field

$$E_s = \frac{-Q_s}{\varepsilon_0 \varepsilon_{rb} S} = \frac{eN\Delta z}{\varepsilon_0 \varepsilon_{rb}} \tag{32.19}$$

which acts on each electron with the force

$$F_s = -eE_s = \frac{-e^2 N \Delta z}{\varepsilon_0 \varepsilon_{rb}} \tag{32.20}$$

that is directed in opposite to the charge motion. The equation of motion is

$$m_0 \frac{d^2(\Delta z)}{dt^2} = -\frac{e^2 N_e \Delta z}{\varepsilon_0 \varepsilon_{rb}} = -\omega_{ps}^2 \Delta z \tag{32.21}$$

And it has a solution

$$\Delta z \sim \Delta z_0 \cos(\omega_{ps} t) \tag{32.22}$$

which is self-sustaining longitudinal collective oscillations of all electrons– plasmons.

Surface plasmon polaritons (SPP)

Consider now the situation what happens at the boundary between a metal ($\varepsilon_r < 0$) and a dielectric ($\varepsilon_r > 0$) as shown in Fig.32.4a.

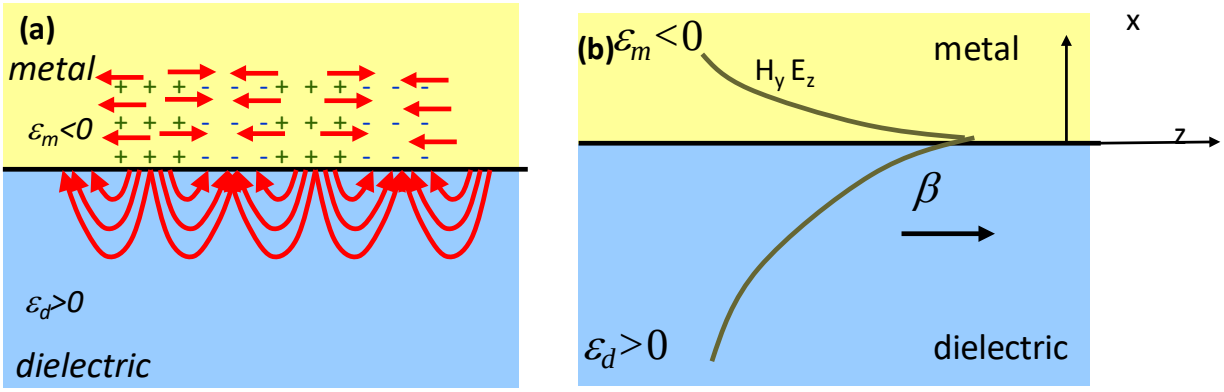

Figure 32.4 (a) Surface plasmon as a coupled wave of charge and field oscillations (b) Fields in propagating surface plasmon polariton (SPP) – surface plasmon coupled to a photon

Now in addition to the field inside the metal there is also a fringe field penetrating the dielectric. It is clear that since part of the field is outside the metal the restoring force is weaker than in the bulk, so one expects that the frequency of the surface plasmon is less than that of bulk plasmon ω_{ps} . Second, the field is no longer strictly longitudinal, therefore the surface plasmon can couple to the propagating photon and thus make up a *surface plasmon polariton (SPP)* . SPP is in fact a TM wave propagating at the metal-dielectric interface as shown in Fig.32.4b. The Maxwell's equation can be written as always as

$$\begin{aligned} \nabla \times \mathbf{H} &= \varepsilon(x) \frac{\partial \mathbf{E}}{\partial t} \\ \nabla \times \mathbf{E} &= -\mu_0 \frac{\partial \mathbf{H}}{\partial t} \end{aligned} \tag{32.23}$$

And since the frequency dependence is harmonic $\exp(j\omega t)$ one can re-write (32.23) as

$$\begin{aligned}
&\frac{\partial H_y}{\partial z} = j\omega\varepsilon(x)E_x \\
&\frac{\partial H_x}{\partial z} - \frac{\partial H_z}{\partial x} = -j\omega\varepsilon(x)E_y \\
&\frac{\partial H_y}{\partial x} = -j\omega\varepsilon(x)E_z \\
&\frac{\partial E_y}{\partial z} = -j\omega\mu H_x \\
&\frac{\partial E_x}{\partial z} - \frac{\partial E_z}{\partial x} = j\omega\mu H_y \\
&\frac{\partial E_y}{\partial x} = j\omega\mu H_z
\end{aligned} \tag{32.24}$$

From the first, third, and fifth equations in (32.24) we readily obtain the TM solution

$$\begin{aligned}
&\mathbf{H} = H_y\hat{\mathbf{y}} \\
&E_x = -\frac{j}{\omega\varepsilon(x)}\frac{\partial H_y}{\partial z} \\
&E_z = \frac{j}{\omega\varepsilon(x)}\frac{\partial H_y}{\partial x}
\end{aligned} \tag{32.25}$$

Since the magnetic field is harmonic

$$H_y(x,z,t) = \mathrm{H}(x)e^{j(\beta z-\omega t)} \tag{32.26}$$

the wave equation is

$$\frac{d^2H}{dx^2} + \frac{d^2H}{dz^2} + \frac{\omega^2}{c^2}\varepsilon_r(x) = 0 \tag{32.27}$$

We consider the wave that is evanescent in both metal and dielectric, i.e.

$$\begin{aligned}
&\mathrm{H}(x>0) = H_0e^{-q_mx} \\
&\mathrm{H}(x<0) = H_0e^{q_dx}
\end{aligned} \tag{32.28}$$

as shown in Fig.34.4b. Substituting into (32.27) one gets

$$\begin{aligned}
&q_m^2 - \beta^2 = -\varepsilon_m k_0^2 = |\,\varepsilon_m\,|\,k_0^2 \\
&q_d^2 - \beta^2 = -\varepsilon_d k_0^2
\end{aligned} \tag{32.29}$$

where of course $k_0 = \omega/c$ .Re-write (32.29) as

$$q_m = \sqrt{|\varepsilon_m| k_0^2 + \beta^2}$$
$$q_d = \sqrt{\beta^2 - \varepsilon_d k_0^2} \tag{32.30}$$

Subtract the second line in (32.29) from the first one to get the relation between two transverse decay cosntants

$$q_m^2 - q_d^2 = \left(|\varepsilon_m| + \varepsilon_d\right) k_0^2 \tag{32.31}$$

Now, according to the last equation in (32.25) the longitudinal E field is

$$E_z = \begin{cases} -\dfrac{jq_m H_0 e^{j(\beta z - \omega t)} e^{-q_m x}}{\omega \varepsilon_0 \varepsilon_m} & x > 0 \\ \dfrac{jq_d H_0 e^{j(\beta z - \omega t)} e^{q_d x}}{\omega \varepsilon_0 \varepsilon_d} & x < 0 \end{cases} \tag{32.32}$$

Since E_z is continuous we obtain

$$\frac{q_m}{q_d} = -\frac{\varepsilon_m}{\varepsilon_d} = \frac{|\varepsilon_m|}{\varepsilon_d} \tag{32.33}$$

Substitute (32.33) into (32.31)

$$q_d^2 \left(\frac{|\varepsilon_m|}{\varepsilon_d}\right)^2 - q_d^2 = \left(|\varepsilon_m| + \varepsilon_d\right) k_0^2 \tag{32.34}$$

And finally

$$\frac{q_d^2}{k_0^2} = \frac{|\varepsilon_m| + \varepsilon_d}{|\varepsilon_m|^2 - \varepsilon_d^2} \varepsilon_d^2 = \frac{\varepsilon_d^2}{|\varepsilon_m| - \varepsilon_d} \tag{32.35}$$

Therefore

$$q_d = k_0 \sqrt{\frac{\varepsilon_d^2}{|\varepsilon_m| - \varepsilon_d}} = k_0 n_d \sqrt{\frac{\varepsilon_d}{|\varepsilon_m| - \varepsilon_d}} \tag{32.36}$$

and

$$q_m = k_0 \sqrt{\frac{|\varepsilon_m|^2}{|\varepsilon_m| - \varepsilon_d}} = k_0 |\varepsilon_m|^{1/2} \sqrt{\frac{|\varepsilon_m|}{|\varepsilon_m| - \varepsilon_d}} \tag{32.37}$$

Substituting (32.36) and (32.37) into (32.29) we finally obtain

$$\beta^2 = \varepsilon_d k_0^2 + q_d^2 = k_0^2 \left[\frac{\varepsilon_d^2}{|\varepsilon_m| - \varepsilon_d} + \varepsilon_d\right] = \varepsilon_d k_0^2 \frac{|\varepsilon_m|}{|\varepsilon_m| - \varepsilon_d} \tag{32.38}$$

No we have the depression for the the propagation constant of SPP.

$$\beta = n_d k_0 \sqrt{\frac{|\varepsilon_m|}{|\varepsilon_m| - \varepsilon_d}} = n_d k_0 \sqrt{\frac{\varepsilon_m}{\varepsilon_m + \varepsilon_d}} \tag{32.39}$$

And the effective index is

$$n_{eff} = n_d \sqrt{\frac{\varepsilon_m}{\varepsilon_m + \varepsilon_d}} > n_d \tag{32.40}$$

As one can see when $\varepsilon_m = -\varepsilon_d$, $\beta \to \infty$ i.e. the wavelength of SPP becomes infinitely short, and, furthermore, $q_m, q_d \to \infty$-the SPP gets localized in a very small sub-wavelength layer near the interface.

Dispersion law of the SPP

I few now insert the expression for the metal (32.3) (without damping) into (32.39) we obtain

$$\beta(\omega) = n_d k_0 \sqrt{\frac{|\varepsilon_m|}{|\varepsilon_m| - \varepsilon_d}} = n_d k_0 \sqrt{\frac{\frac{\omega_p^2}{\omega^2} - \varepsilon_{rb}}{\frac{\omega_p^2}{\omega^2} - \varepsilon_{rb} - \varepsilon_d}} = n_d \frac{\omega}{c} \sqrt{\frac{\omega_p^2 - \varepsilon_{rb}\omega^2}{\omega_p^2 - (\varepsilon_{rb} + \varepsilon_d)\omega^2}} = \tag{32.41}$$

$$= n_d \frac{\omega}{c} \sqrt{1 + \frac{\omega^2 \varepsilon_d}{\omega_p^2 - (\varepsilon_d + \varepsilon_{rb})\omega^2}} = n_d \frac{\omega}{c} \sqrt{1 + \frac{1}{\varepsilon_{rb}/\varepsilon_d + 1} \frac{\omega^2}{\omega_{sp}^2 - \omega^2}}$$

Where we have introduced surface plasmon resonance

$$\omega_{sp} = \frac{\omega_p}{\sqrt{\varepsilon_d + \varepsilon_{rb}}} = \frac{\omega_{ps}}{\sqrt{1 + \varepsilon_d / \varepsilon_{rb}}} \tag{32.42}$$

Note that I the dielectric is vacuum and also $\varepsilon_{rb} = 1$ then $\omega_{sp} = \omega_p / \sqrt{2}$. Indeed, the SP resonance frequency is less than frequency of bulk plasmon sine the field fringes outside the metal so the restoring force acting on electron is weaker. The dispersion curve is plotted in Fig.35.5(a).

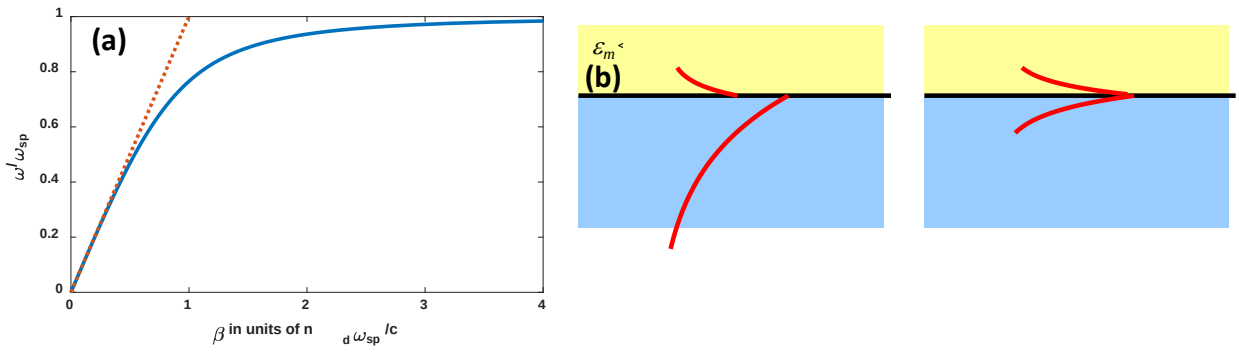

Figure 32.5 (a) SPP dispersion curve (in the absence of losses) (b) field from SP resonance (c) field close to SP resonance.

Note that far the SP resonance frequency, i.e. $\omega << \omega_{sp}$ the second term under the square root in (32.41) is much less than 1, so that

$$\beta \approx n_d \frac{\omega}{c} \tag{32.43}$$

And the dispersion is linear, or photon-like. Also since according to (32.3) for low frequencies metal has very large negative dielectric constant $|\varepsilon_m| >> \varepsilon_d$, according to (32.33) $q_m >> q_d$ and most of the electric field is contained in the dielectric as shown in Fig.32.5b

At the other extreme, close to the SP resonance $\omega \to \omega_{sp}$ the propagating constant diverges

$$\beta \simeq n_d \frac{\omega}{c} \sqrt{\frac{1}{2(\varepsilon_{rb}/\varepsilon_d + 1)} \frac{\omega}{\omega_{sp} - \omega}} \tag{32.44}$$

and also, since $|\varepsilon_m| \approx \varepsilon_d$ the electric field penetrates metal and dielectric equally as shown in Fig.32c .

SPP characteristics

Let us estimate the *effective width* of the SPP as, for instance,

$$W_{eff} = q_m^{-1} + q_d^{-1} \tag{32.45}$$

Substituting (32.36) and (32.37) we get

$$W_{eff} = \left[k_0 \sqrt{\frac{\varepsilon_d^2}{|\varepsilon_m| - \varepsilon_d}} \right]^{-1} + \left[k_0 \sqrt{\frac{|\varepsilon_m|^2}{|\varepsilon_m| - \varepsilon_d}} \right]^{-1} = \frac{\lambda}{2\pi} \sqrt{|\varepsilon_m| - \varepsilon_d} \left[\frac{1}{\varepsilon_d} + \frac{1}{|\varepsilon_m|} \right] = \frac{\lambda}{2\pi n_d} \sqrt{\frac{|\varepsilon_m|}{\varepsilon_d} - 1} \left(1 + \frac{\varepsilon_d}{|\varepsilon_m|} \right) \tag{32.46}$$

As shown in Fig.32.6a far from SP resonance, when $|\varepsilon_m| >> \varepsilon_d$ effective width is large

$$W_{eff} \approx \frac{\lambda |\varepsilon_m|^{1/2}}{2\pi\varepsilon_d} \tag{32.47}$$

But close to SPP resonance it goes to zero as

$$W_{eff} \approx \frac{\lambda}{\pi n_d} \sqrt{\frac{|\varepsilon_m|}{\varepsilon_d} - 1} \tag{32.48}$$

Next, consider the group velocity of SPP (or, better, the inverse of it) and differentiate (32.41)

$$v_g^{-1} = \frac{d\beta}{d\omega} = \frac{n_d}{c}\sqrt{1+\frac{1}{\varepsilon_{rb}/\varepsilon_d+1}\frac{\omega^2}{\omega_{sp}^2-\omega^2}} + \frac{n_d}{c}\frac{\frac{1}{\varepsilon_{rb}/\varepsilon_d+1}}{\sqrt{1+\frac{1}{\varepsilon_{rb}/\varepsilon_d+1}\frac{\omega^2}{\omega_{sp}^2-\omega^2}}}\frac{\omega^2\omega_{sp}^2}{\left[\omega_{sp}^2-\omega^2\right]^2} \quad (32.49)$$

This curve is shown in Fig. 32.6bNote that v_g^{-1} diverges much stronger than β in the vicinity of SPP resonance due to the presence of the last term in (32.49). Indeed for $\omega \to \omega_{sp}$

$$v_g^{-1} = \frac{n_d}{c}\sqrt{\frac{1}{\varepsilon_{rb}/\varepsilon_d+1}\frac{\omega^2}{\omega_{sp}^2-\omega^2}} + \frac{n_d}{c}\frac{1}{\sqrt{\varepsilon_{rb}/\varepsilon_d+1}}\frac{\omega\omega_{sp}^2}{\left[\omega_{sp}^2-\omega^2\right]^{3/2}} = \frac{n_d}{c}\frac{\omega}{\sqrt{\varepsilon_{rb}/\varepsilon_d+1}}\left[\frac{1}{\left(\omega_{sp}^2-\omega^2\right)^{1/2}}+\frac{\omega_{sp}^2}{\left(\omega_{sp}^2-\omega^2\right)^{3/2}}\right] \quad (32.50)$$

As $\omega \to \omega_{sp}$ the second term dominates and using (32.44) we can see that $v_g \sim \beta^{-3}$

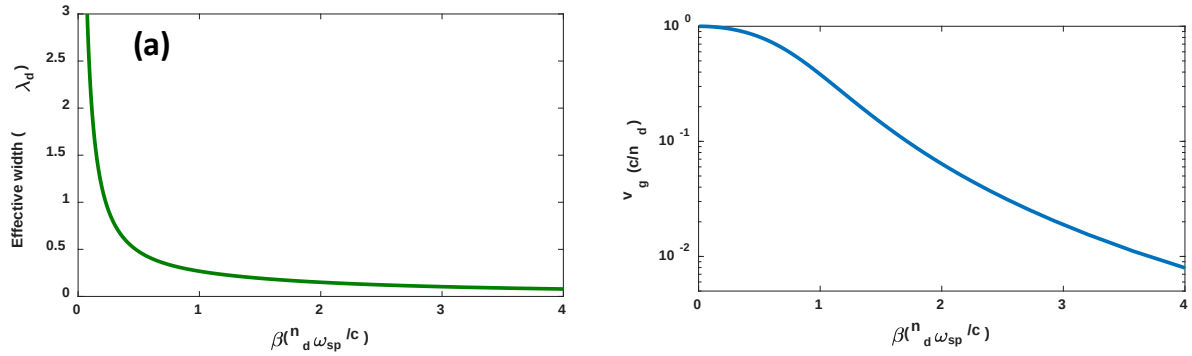

Figure 32.6 (a) Effective width and (b) Group velocity of SPP versus propagation constant

Why SPP is a slow wave?

To understand it, look at the Fig.32.7 where the fields and Poynting vectors are shown in metal and dielectrics. The key factor is that normal electric field E_x changes sign at the boundary, with the relation

$$\left|\varepsilon_m E_{x,m}\right| = \left|\varepsilon_d E_{x,d}\right| \quad (32.51)$$

Therefore, Poynting vector in the metal is opposite to the direction of propagation.

$$\begin{aligned} S_d &= \frac{1}{2}H_0 E_{xd} \\ S_m &= \frac{1}{2}H_0 E_{xm} = -\frac{1}{2}H_0 E_d \frac{\varepsilon_d}{|\varepsilon_m|} \end{aligned} \quad (32.52)$$

The total propagating power is

$$P = W\left[\int S_d dx + \int S_m dx\right] \tag{32.53}$$

where W is the width along y direction. Integration of exponentially decaying as *-2wx* variables yields

$$P = \frac{W}{2q_d}\frac{1}{2}\left|H_0 E_{xd}\right| - \frac{W}{2q_m}\frac{1}{2}\left|H_0 E_{xm}\right| = W\frac{S_d}{2q_d}\left(1 - \frac{q_d}{q_m}\frac{\varepsilon_d}{|\varepsilon_m|}\right) = W\frac{S_d}{2q_d}\left(1 - \frac{\varepsilon_d^2}{|\varepsilon_m|^2}\right) \tag{32.54}$$

Obviously near SP resonance $P \to 0$. One half of the energy is in the metal and the other half is in dielectric – as they propagate in the opposite directions there is no net motion of energy.

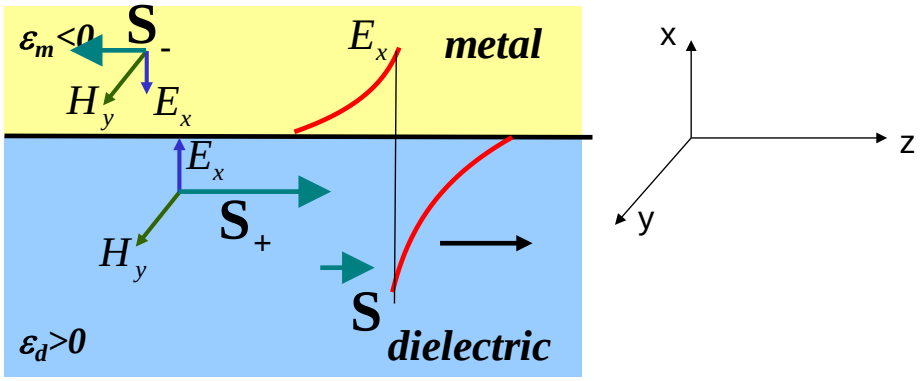

Figure 32.7 Poynting vector in SPP

SPP polarization

The difference in the sign of dielectric constant also has interesting consequences for the polarization properties of the SPP. Using (32.24) we can write for continuous longitudinal electric field in two media

$$E_z = \begin{cases} -\dfrac{jq_m H_0 e^{j(\beta z-\omega t)} e^{-q_m x}}{\omega\varepsilon_0\varepsilon_m} & x > 0 \\ \dfrac{jq_d H_0 e^{j(\beta z-\omega t)} e^{q_d x}}{\omega\varepsilon_0\varepsilon_d} & x < 0 \end{cases} \tag{32.55}$$

and for the discontinuous transverse electric field

$$E_x = -\frac{j}{\omega\varepsilon_0\varepsilon_r(x)}\frac{\partial H_y}{\partial z} = \begin{cases} \dfrac{\beta H_0 e^{j(\beta z-\omega t)} e^{-q_m x}}{\omega\varepsilon_0\varepsilon_m} & x > 0 \\ \dfrac{\beta H_0 e^{j(\beta z-\omega t)} e^{q_d x}}{\omega\varepsilon_0\varepsilon_d} & x < 0 \end{cases} \tag{32.56}$$

As one can see in the metal(dielectric) transverse field is 90 degrees behind (in front) of the longitudinal field, i.e. the electric field rotates counterclockwise (clockwise) as shown in Fig. 32.8a. One can say that it is "elliptically polarized" in the "longitudinal" xz plane. One can also obtain the expressions for the half-axes of the ellipses from (32.55) and (32.56) using the expressions (32.36)-(32.38)

$$\left|\frac{E_z}{E_x}\right| = \begin{cases} q_m/\beta = \sqrt{|\varepsilon_m|/\varepsilon_d} & x>0 \\ q_d/\beta = \sqrt{\varepsilon_d/|\varepsilon_m|} & x<0 \end{cases} \tag{32.57}$$

These ratios are plotted in Fig.32.8b. It is easy to observe that far from SP resonance

$$\begin{aligned} \left|\frac{E_z}{E_x}\right| &>> 1 \quad x>0 \\ \left|\frac{E_z}{E_x}\right| &<< 1 \quad x<0 \end{aligned} \tag{32.58}$$

i.e.the ellipses have very high eccentricity and the polarization is practically linear – transverse (as expected for a photon) in the dielectric and longitudinal (as expected for a plasmon) in the metal. But as one approaches SP resonance $|\varepsilon_m| \to \varepsilon_d$ and the polarization becomes nearly circular both in metal and dielectric.

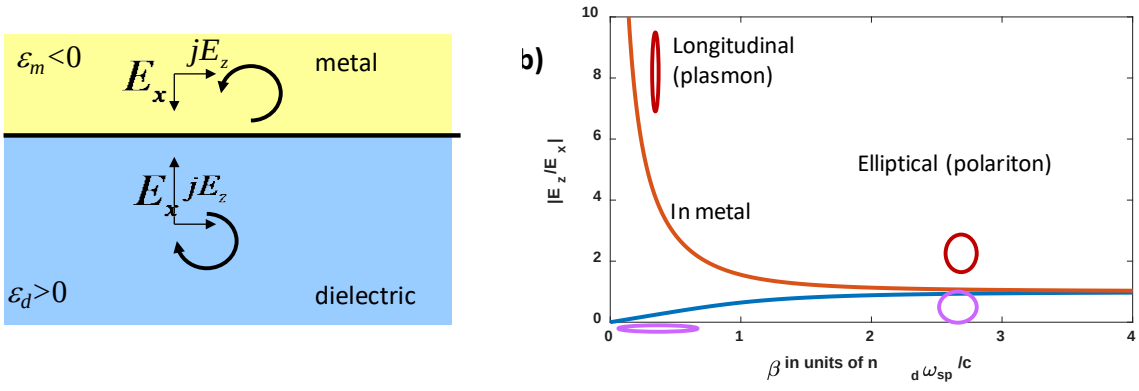

Figure 32.8 (a) polarization of SPP (b) ratio of two field components in SPP vs. propagation constant

Effective impedance of SPP

Let us find re-work the expression for the electric fields in the dielectric and metal. From (32.55)

$$\left|\frac{E_z}{H_0}\right| = \frac{q_d}{\omega\varepsilon_0\varepsilon_d} = \frac{q_d}{n_d k_0}\frac{k_0}{\omega\varepsilon_0 n_d} = \frac{q_d}{n_d k_0}\frac{1}{c\varepsilon_0 n_d} = \frac{q_d}{n_d k_0}\frac{\eta_0}{n_d} = \frac{q_d}{n_d k_0}\eta_d \tag{32.59}$$

Also we can write for metal and dielectric

$$\begin{aligned} \left|\frac{E_{xd}}{H_0}\right| &= \frac{\beta}{\omega\varepsilon_0\varepsilon_d} = \frac{\beta}{n_d k_0}\frac{\eta_0}{n_d} = \frac{\beta}{n_d k_0}\eta_d \\ \left|\frac{E_{xm}}{H_0}\right| &= \frac{\beta}{n_d k_0}\frac{\varepsilon_d}{|\varepsilon_m|}\eta_d \end{aligned} \tag{32.60}$$

Now, the total electric field sin dielectric and metal are

$$E_d = \sqrt{\left|E_{x,d}\right|^2 + \left|E_{z,d}\right|^2} = \frac{\sqrt{q_d^2 + \beta^2}}{n_d k_0}\eta_d H_0 = \eta_{SPP} H_0$$
$$E_m = \sqrt{\left|E_{x,m}\right|^2 + \left|E_{z,m}\right|^2} = \frac{\sqrt{q_d^2 + \beta^2 \varepsilon_d^2 / |\varepsilon_m|^2}}{n_d k_0} H_0 = \eta_{SPP}^{'} H_0 \quad (32.61)$$

Where we have introduced effective impedances for SPP in metal and dielectric

$$\eta_{SPP} = \frac{\sqrt{q_d^2 + \beta^2}}{n_d k_0}\eta_d = \frac{1}{n_d}\sqrt{\frac{\varepsilon_d^2 + \varepsilon_d |\varepsilon_m|}{|\varepsilon_m| - \varepsilon_d}}\eta_d = \sqrt{\frac{|\varepsilon_m| + \varepsilon_d}{|\varepsilon_m| - \varepsilon_d}}\eta_d$$
$$\eta_{SPP}^{'} = \frac{\sqrt{q_d^2 + \beta^2 \varepsilon_d^2 / |\varepsilon_m|^2}}{n_d k_0}\eta_d = \frac{1}{n_d}\sqrt{\frac{\varepsilon_d^2 + \varepsilon_d^3 / |\varepsilon_m|}{|\varepsilon_m| - \varepsilon_d}}\eta_d = \sqrt{\frac{\varepsilon_d + \varepsilon_d^2 / |\varepsilon_m|}{|\varepsilon_m| - \varepsilon_d}}\eta_d \quad (32.62)$$

We can now find the ratio of two impedances

$$\frac{\eta_{SPP}^{'}}{\eta_{SPP}} = \sqrt{\frac{\varepsilon_d + \varepsilon_d^2 / |\varepsilon_m|}{\varepsilon_d + |\varepsilon_m|}} = \sqrt{\frac{\varepsilon_d}{|\varepsilon_m|}\frac{|\varepsilon_m| + \varepsilon_d}{\varepsilon_d + |\varepsilon_m|}} = \sqrt{\frac{\varepsilon_d}{|\varepsilon_m|}} \quad (32.63)$$

The results are plotted in Fig. 32.9. It is easy to see that far from SPP resonance $|\varepsilon_m| >> \varepsilon_d$ so that

$$\eta_{SPP} \approx \eta_d$$
$$\eta_{SPP}^{'} \approx \frac{\varepsilon_d}{|\varepsilon_m|}\eta_d << \eta_d \quad (32.64)$$

Which makes perfect sense – in dielectric one has essentially a photon propagating so the impedance es that of dielectric and in the metal one has no electric field so the impedance is very small. One can define mean impedance by weighing two impedances according to the fraction of energy in metal and dielectric. Far from SPP obviously it is just η_{SPP} .But near SP resonance $\omega \to \omega_{sp}$ both impedances become large and obviously nearly equal. Since when $|\varepsilon_m| \to \varepsilon_d$ we have

$$q_m \approx q_d \approx \beta \quad (32.65)$$

the expression for effective impedance becomes

$$\eta_{SPP} \approx \eta_{SPP}^{'} \approx \frac{\beta\sqrt{2}}{n_d k_0}\eta_d \quad (32.66)$$

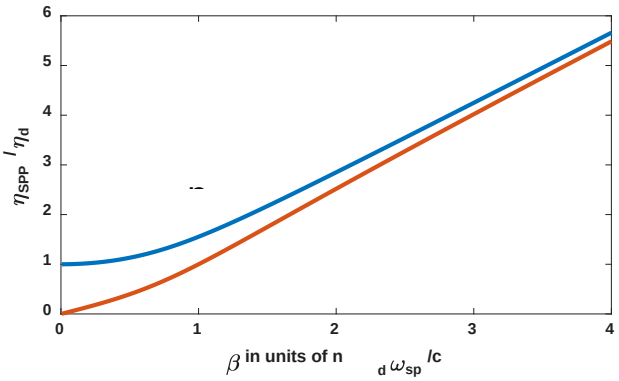

Figure 32.9 Effective impedance of SPP in the dielectric and metal.

So, large propagation constant (sub-diffraction limit) SPP's have large effective impedance and therefore it is difficult to couple the light in and out of such SPP because of the impedance mismatch.

Energy of the SPP

Let us now find the energy densities in dielectric and metal, per unit of the surface are, Magentic surface energy density in the dielectric

$$U_{M,d} = \frac{1}{4}\mu_0 H_0^2 \int_{-\infty}^{0} e^{-2q_d x} dx = \frac{1}{8q_d}\mu_0 H_0^2 \tag{32.67}$$

and in metal it is

$$U_{M,m} = \frac{1}{4}\mu_0 H_0^2 \int_{0}^{\infty} e^{-2q_m x} dx = \frac{1}{8q_m}\mu_0 H_0^2 \tag{32.68}$$

The electric surface energy density in the dielectric is

$$U_{E,d} = \frac{1}{8q_d}\varepsilon_0\varepsilon_d\left(\left|E_{x,d}\right|^2 + \left|E_{z,d}\right|^2\right) = \frac{1}{8q_d}\varepsilon_0\varepsilon_d\eta_{SPP}^2 H_0^2 \tag{32.69}$$

while in the metal, which is highly dispersive it is

$$U_{E,m} = \frac{1}{8q_m}\varepsilon_0\frac{d\left(\omega\varepsilon_m\right)}{d\omega}\left(\left|E_{x,d}\right|^2 + \left|E_{z,d}\right|^2\right) = \frac{1}{8q_m}\varepsilon_0\frac{d\left(\omega\varepsilon_m\right)}{d\omega}\frac{\varepsilon_d}{|\varepsilon_m|}\eta_{SPP}^2 H_0^2 \tag{32.70}$$

where we have used (32.63). Let us now find the dispersive term using (32.3) (without damping)

$$\frac{d\left(\omega\varepsilon_m\right)}{d\omega} = \varepsilon_{rb} - \frac{\omega_p^2}{\omega^2} + \omega\frac{d\left(\varepsilon_{rb} - \omega_p^2/\omega^2\right)}{d\omega} = \varepsilon_{rb} - \frac{\omega_p^2}{\omega^2} + 2\frac{\omega_p^2}{\omega^2} = \frac{\omega_p^2}{\omega^2} - \varepsilon_{rb} + 2\varepsilon_{rb} = |\varepsilon_m| + 2\varepsilon_{rb} \tag{32.71}$$

Therefore,

$$U_{E,m} = \frac{1}{8q_m}\varepsilon_0\varepsilon_d(1+2\varepsilon_{rb}/|\varepsilon_m|)\eta_{SPP}^2 H_0^2 \tag{32.72}$$

We can normalize all the energies to the electric energy density in the dielectric (32.69):

$$\begin{aligned} U_{E,m} &= \frac{q_d}{q_m}(1+2\varepsilon_{rb}/|\varepsilon_m|)U_{E,d} = \frac{\varepsilon_d}{|\varepsilon_m|}(1+2\varepsilon_{rb}/|\varepsilon_m|)U_{E,d} \\ U_{M,d} &= \frac{\mu_0}{\varepsilon_0\varepsilon_d\eta_{SPP}^2}U_{E,d} = \frac{\mu_0}{\varepsilon_0\varepsilon_d\eta_d^2}\frac{|\varepsilon_m|-\varepsilon_d}{|\varepsilon_m|+\varepsilon_d}U_{E,d} = \frac{|\varepsilon_m|-\varepsilon_d}{|\varepsilon_m|+\varepsilon_d}U_{E,d} \\ U_{M,m} &= \frac{\varepsilon_d}{|\varepsilon_m|}\frac{|\varepsilon_m|-\varepsilon_d}{|\varepsilon_m|+\varepsilon_d}U_{E,d} \end{aligned} \tag{32.73}$$

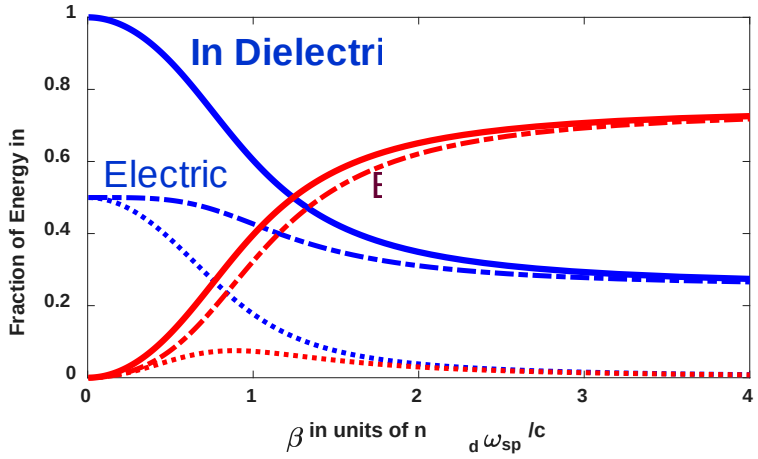

Figure 32.10 Energy balance in the SPP mode

These results are now plotted in Fig.32.10. It is easy to see that far from SP resonance, when $|\varepsilon_m| >> \varepsilon_d$ the fraction energy density in the metal is very small , while the magnetic and electric energy densities in dielectric are equal to each other $U_{E,d} = U_{M,d}$ as expected for a propagating wave in the dielectric. As one approaches SP resonance the energy gets re-distributed. The fraction of energy in metal rises while the magnetic energy decreases. Near SP resonance one has no magnetic energy $U_{M,d} = U_{M,m} = 0$ and also

$$U_{E,m} = (1+2\varepsilon_{rb}/\varepsilon_d)U_{E,d} \tag{32.74}$$

Clearly, more energy is contained in metal now – it has to do with the kinetic energy of free carriers. And that needs to be explored.

Kinect and Potential energies in SPP

Consider electron gas subjected to the electric field $E\cos(\omega t)$ and oscillating at frequency ω, with velocity

$$v(t) = -eE\sin(\omega t)/m_0\omega \tag{32.75}$$

The (volume) density of kinetic energy is

$$u_k(t) = \frac{1}{2} N m_0 v^2(t) = \frac{1}{2} N m_0 \left(\frac{eE}{m_0 \omega} \sin \omega t \right)^2 = \frac{1}{2} \frac{Ne^2}{m_0 \omega^2} E^2 \sin^2 \omega t = \frac{1}{2} \varepsilon_0 \frac{\omega_p^2}{\omega^2} E^2 \sin^2 \omega t \quad (32.76)$$

and averaging over the time yields

$$\left\langle u_k(t) \right\rangle_t = \frac{1}{4} \varepsilon_0 \frac{\omega_p^2}{\omega^2} E_m^2 \quad (32.77)$$

Let us re-write the expression for the electrical energy density in metal (32.73) as

$$U_{E,m} = \frac{\varepsilon_d}{|\varepsilon_m|}(1 + \varepsilon_{rb} / |\varepsilon_m| + \varepsilon_{rb} / |\varepsilon_m|) U_{E,d} = \frac{\varepsilon_d}{|\varepsilon_m|^2}(|\varepsilon_m| + \varepsilon_{rb}) U_{E,d} + \frac{\varepsilon_d}{|\varepsilon_m|^2} \varepsilon_{rb} U_{E,d} = \frac{\varepsilon_d}{|\varepsilon_m|^2} \frac{\omega_p^2}{\omega^2} U_{E,d} + \frac{\varepsilon_d \varepsilon_{rb}}{|\varepsilon_m|^2} U_{E,d} \quad (32.78)$$

The first term clearly corresponds to the kinetic energy of free electrons oscillating as $\sin^2 \omega t$

$$U_K = \frac{\varepsilon_d}{|\varepsilon_m|}(1 + \varepsilon_{rb} / |\varepsilon_m|) U_{E,d} \quad (32.79)$$

While the second term is “electric energy” that includes electric field energy in vacuum and potential energy of the valence electrons (polarization oscillations), both oscillating as $\cos^2 \omega t$, i..e in-phase with the electric field

$$U_{E,mP} = \frac{\varepsilon_d \varepsilon_{rb}}{|\varepsilon_m|^2} U_{E,d} \quad (32.80)$$

Therefore, the total in-phase electric energy is

$$U_E = U_{E,d} + U_{E,mP} = \left(1 + \frac{\varepsilon_d \varepsilon_{rb}}{|\varepsilon_m|^2} \right) U_{E,d} \quad (32.81)$$

In addition to the kinetic energy there is also a magnetic energy, oscillating in-quadrature with the electric as $\sin^2 \omega t$

$$\begin{aligned} U_M &= U_{M,d} + U_{M,m} = \\ &= \left(\frac{\varepsilon_d}{|\varepsilon_m|} + 1 \right) \frac{|\varepsilon_m| - \varepsilon_d}{|\varepsilon_m| + \varepsilon_d} U_{E,d} = \left(1 - \frac{\varepsilon_d}{|\varepsilon_m|} \right) U_{E,d} \end{aligned} \quad (32.82)$$

Hence the total in-quadrature energy is

$$U_Q = U_M + U_K = \left(1 - \frac{\varepsilon_d}{|\varepsilon_m|} + \frac{\varepsilon_d}{|\varepsilon_m|} + \frac{\varepsilon_d \varepsilon_{rb}}{|\varepsilon_m|^2}\right) = \left(1 + \frac{\varepsilon_d \varepsilon_{rb}}{|\varepsilon_m|^2}\right) U_{E,d} = U_E \tag{32.83}$$

That is the perfect energy balance between three energies – one has electric (potential) energy oscillating in phase with the electric field consisting of the energy of electric field in vacuum and bound valence electrons energy in both metal and dielectric. And in quadrature one has kinetic energy of free carriers in the metal plus magnetic field energy. The composition of energy oscillating in quadrature gets changed – far from SP resonance it is all magnetic, but clos eto the SP resonance it is all in kinetic motion of carriers. This can be seen from Fig.32.11 a and b plotted versus propagation constant and frequency respectively. Clearly SPP far from SP resonance behaves as a photon and near SP as a plasmon.

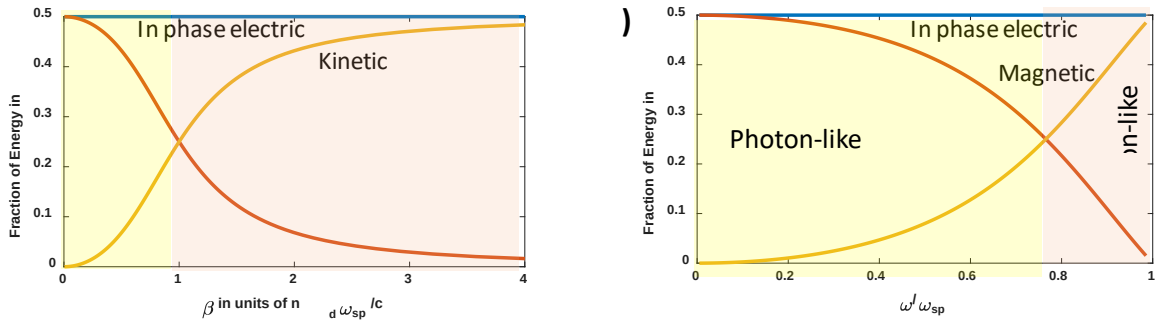

Figure 32.11. Energy balance in SPP (a) vs propagation constant (b) vs. frequency

The important implication is the inevitable high loss in SPP as it approaches resonance. Since nearly ½ of th entire energy is contained in oscillations of free carriers whose velocity (momentum) is subject to the decay with the damping rate γ (hence their kinetic energy decays as 2γ), the energy in the entire SPP mode decays as γ which is of course quite high.

Damping and Propagation Length of SPP

Let us re-introduce the damping γ into the SPP dispersion equation (32.41)

$$\beta = n_d k_0 \sqrt{\frac{\varepsilon_m}{\varepsilon_m + \varepsilon_d}} = n_d \frac{\omega}{c} \sqrt{1 + \frac{1}{\varepsilon_{rb}/\varepsilon_d + 1} \frac{\omega^2 + j\omega\gamma}{\omega_{sp}^2 - \omega^2 - j\omega\gamma}} \tag{32.84}$$

Introduce complex frequency

$$\tilde{\omega}^2 = \omega^2 + j\omega\gamma = \omega^2 + j\omega\gamma + \frac{\gamma^2}{4} - \frac{\gamma^2}{4} \approx \left(\omega + j\frac{\gamma}{2}\right)^2 \tag{32.85}$$

Then

$$\beta(\tilde{\omega}) = n_d \frac{\omega}{c} \sqrt{1 + \frac{1}{\varepsilon_{rb}/\varepsilon_d + 1} \frac{\tilde{\omega}^2}{\omega_{sp}^2 - \tilde{\omega}^2}} \tag{32.86}$$

Use Taylor expansion

$$\beta(\tilde{\omega}) = \beta(\omega,\gamma) \approx \beta(\omega,0) + j\frac{\gamma}{2} n_d \frac{\omega}{c} \frac{d\sqrt{1+\frac{1}{\varepsilon_{rb}/\varepsilon_d+1}\frac{\omega^2}{\omega_{sp}^2-\omega^2}}}{d\omega} \tag{32.87}$$

Using (32.49) it is easy to see that

$$\beta(\omega,\gamma) = \beta(\omega,0) + j\frac{\gamma}{2}\left[\frac{d\beta}{d\omega} - \frac{\beta}{\omega}\right] = j\frac{\gamma}{2}\left[\frac{1}{v_g} - \frac{1}{v_p}\right] \tag{32.88}$$

The power flow in the SPP is

$$P(z) = P_0 e^{-2\beta_{im} z} = P_0 e^{-z/L_{SPP}} \tag{32.89}$$

Where the propagation length is

$$L_{SPP} = 1/2\beta_{im} = v_g/\gamma[1 - v_g/v_p] \tag{32.90}$$

Since for large β (close to ω_{sp}) $v_g >> v_p$, we have $L_{SPP} \to v_g/\gamma$ which of course makes perfect case- the SPP decays in time with rate γ, hence it decays in space as γ/v_g. The dispersion of real and imaginary parts of propagation constant are shown in Fig. 32.12a.

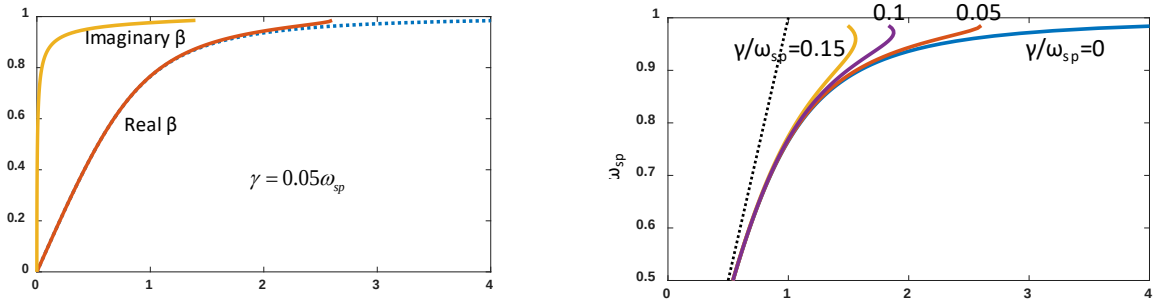

Figure 32.12 (a)Dispersion of real and imaginary propagation constant- first order approximation b) SPP dispersion – exact for different values of damping constant

The relations derived above are actually only approximate and fail very close to SP resonance as shown in Fig. 32.12b. Close to SP resonance the dispersion curve "bends backward" in the presence of loss, because the optical mode resists going into high loss region. This can be seen in Fig.32.12b where Eq. (32.84) (real part) is plotted exactly. One can estimate the maximum attainable value of β by assuming $\omega \approx \omega_{sp}$ in (32.84):

$$\beta_{\max} = n_d \frac{\omega}{c}\sqrt{1+\frac{j}{\varepsilon_{rb}/\varepsilon_d+1}\frac{\omega_{sp}}{\gamma}} \tag{32.91}$$

Assuming that $\lambda_{sp} = 600nm$ ($\omega_{sp} \approx 2\pi \times 5 \times 10^{14} s^{-1}$) we have for Au/air interface $\gamma \approx 1.2 \times 10^{14} s^{-1}$, $\omega/\gamma \sim 25$, and $\beta_{\max} \sim (2.5 + 2.3j) n_d \frac{\omega}{c}$. Fo Ag/air $\gamma \approx .35 \times 10^{14} s^{-1}$ $\omega/\gamma \sim 90$ and $\beta_{\max} \sim (4.8 + 4.7j) n_d \frac{\omega}{c}$, but it is never observed as silver easily oxidizes. Therefore, SPP cannot have really enormous propagation constant. It is limited by optical loss (damping). To illustrate it we plot SPP propagation length for Ag and Au versus wavelength as well as effective index in Fig.32.13 a . As one can see, far from resonance SPP has long propagation length, but it has wavelength practically the same as in dielectric waveguide and it does not offer good confinement. Closer to SP resonance the confinement and effective index increase…but propagation length becomes very short. Even if one introduces a specific figure of merit as

$$FOM = \frac{L_{SPP}}{\lambda_{SPP}} = \frac{\beta_r}{4\pi\beta_{im}} \tag{32.92}$$

the situation does not change significantly – see Fig. 32.13b

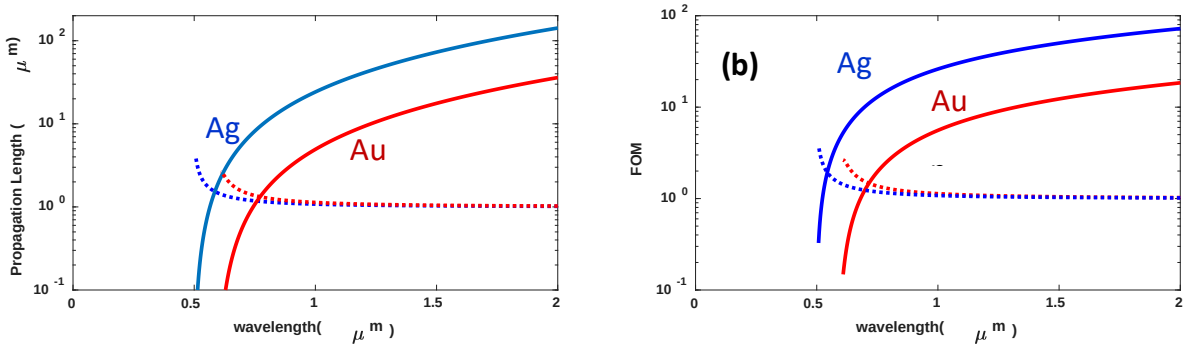

Figure 32.13 (a) SPP propagation length and effective index and (b) Figure of merit and effective index vs. wavelength for Au and Ag

SPP excitation

The wavevector of SPP β_{SPP} is always larger than the maximum, wavevector that can propagate in the dielectric on the interface $k_0 n_d$ as can be seen from (32.41) and Fig.32.5. Therefore, one needs to introduce medium with a higher refractive index such that $n_2 > n_{eff} > n_d$ on the other side of the metal fild, as shown in Fig.31.14 (a) in the so-called Kretschmann configuration where the second medium is fashioned into a prism . When the light propagates in the prism and hits the back metal interface at an incident angle θ its projection at the axis z is $k_z = k_0 n_2 \sin\theta$. When this projection equals the wavevector of SPP β_{SPP} (as shown in Fig. 32.14 b and c) the light couples into the SPP mode,. Otherwise the light simply gets totally reflected since $n_2 \sin\theta > n_d$. The matching condition is

$$k_z = \frac{\omega}{c} n_2 \sin\theta = \frac{\omega}{c} n_d \sqrt{\frac{|\varepsilon_m(\omega)|}{\varepsilon_m(\omega) + n_d^2}} = \beta_{SPP}, \tag{32.93}$$

or

$$\sin\theta = \frac{n_d}{n_2}\sqrt{\frac{|\varepsilon_m(\omega)|}{\varepsilon_m(\omega)+n_d^2}} \tag{32.94}$$

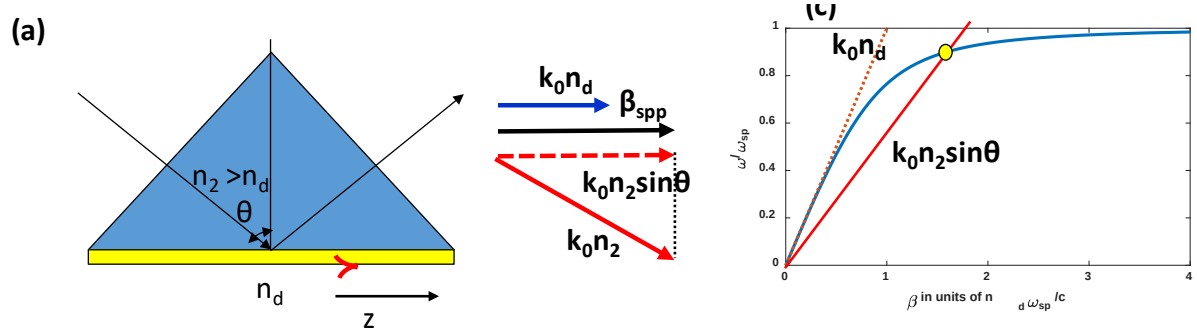

δn **Figure 32.14** (a) Kretschmann configuration for launching SPP. (b) Wavevector matching condition (c) dispersion diagram illustrating wavevector matching

As the light gets coupled into SPP, less of it gets reflected and one can observe a dip of the reflection for p-polarized light as shown in Fig.32.15a

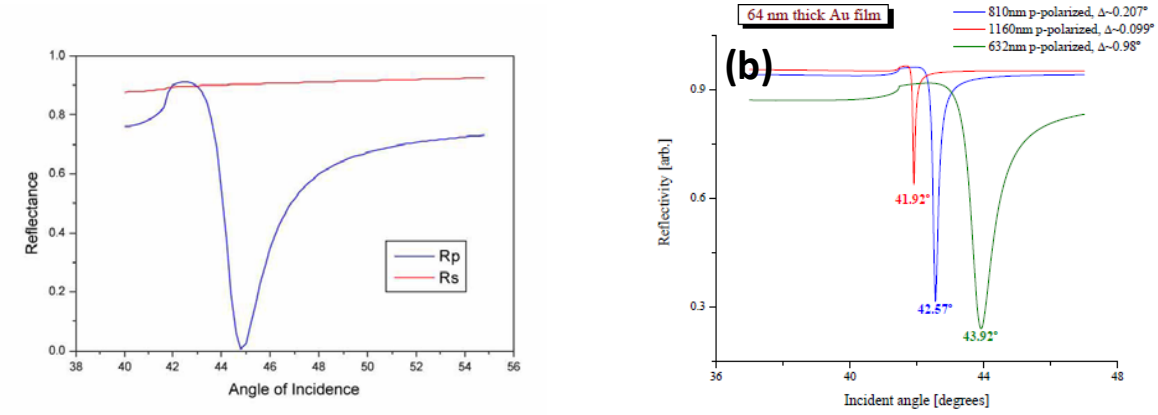

Figure 32.15 (a) Reflectance of S and P polarized light vs. angle in Kretschmann configuration (b) Reflectance for three different wavelengths.

In Fig.32.15 b the reflectivity vs. angle is shown for 3 different wavelengths – clearly one can use this arrangement for sensing the wavelength. But one can also use it to sense the changes in the refractive index.

Plasmonic Sensing

Consider standard the Kretschmann configuration in Fig. 32.16 a in which the index of refraction n_d (typically this is a liquid medium) is changed by a small amount δn - then the reflectivity resonance shifts by a small but distinguishable angle $\delta\theta$ as shown in Fig.32.16b. The key here is the fact that the index is sensed only in a very thin layer – penetration depth of SPP into the dielectric medium. In fact, if one looks at the distribution of electric field inside, as one can see from Fig. 32.16c , it gets enhanced near the

interface inside the dielectric at resonance (mostly from boundary condition of p-polarized light) The amount of field enhancement vs. angle is shown in Fig.32.16d – it is indeed a sharp resonance and the enhancement in energy density approaches 50-fold Therefore, one can also use plasmonic arrangement for fluorescence sensing when we excite only the molecules close to the interface.

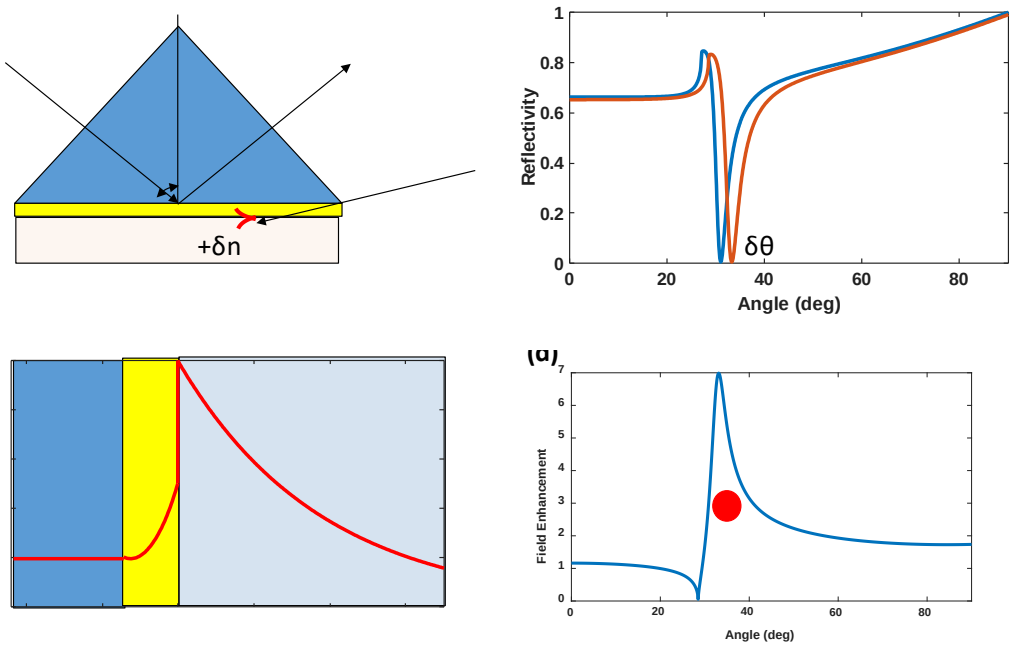

Figure 32.16 (a) small change of index in Kretschmann configuration (b) shift of resonance caused by it (c) Field distribution at resonance (d) resonant enhancement of the electric field

In Fig.32.17 a few examples of different plasmonic biosensors are shown.

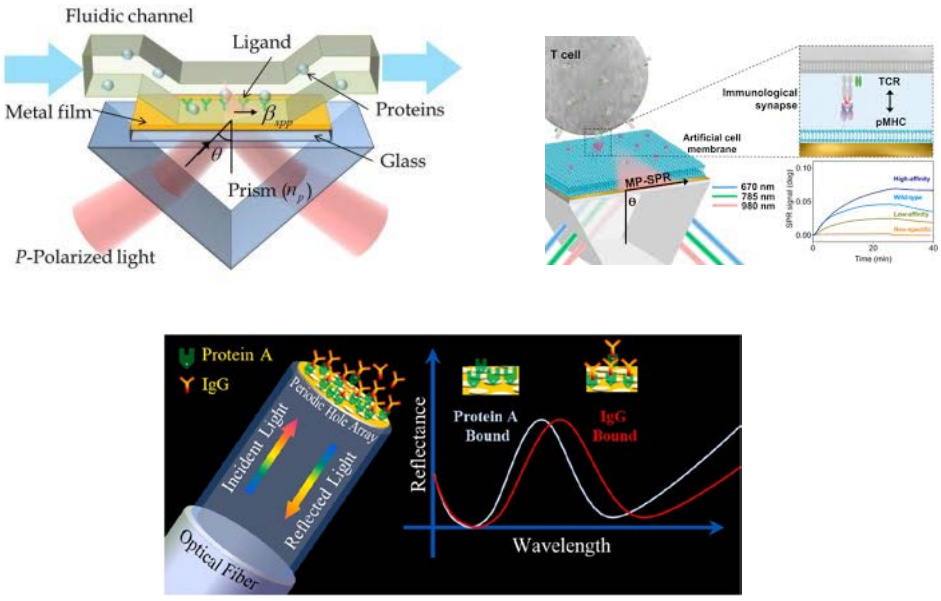

Figure 32.17 Examples of plasmonic sensors

Finally, various alternative methods of SPP excitations are shown in Fig.32.18 In principle any small feature on the surface will have large spatial frequency components in its spatial Fourier transform and these large “wave vectors” will allow momentum matching. So one can use short period grating, or just any sharp feature, such as a tip.

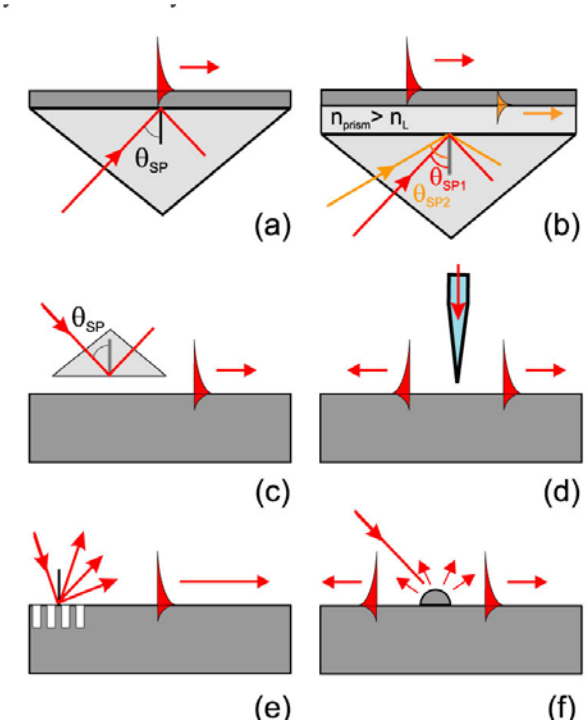

Figure 32.18 SPP excitation configurations (a) Kretschmann geometry (b) two-layer Kretschmann geometry (c) Otto geometry (d) excitation with NSOM probe (e) diffraction on grating (f) diffraction on surface features.